Supplementary Information

Photocatalytically active metal-organic derived ensembles for organic pollutants degradation.

Clara López-García,[a] Celia Castillo-Blas,[a] Marta Iglesias,[a] M. Angeles Monge,[a] Enrique Gutiérrez-Puebla,[a]* Felipe Gándara [a]*

[a] Materials Science Institute of Madrid – Spanish National Research Council (ICMM-CSIC), C/ Sor Juana Inés de la Cruz 3, 28049, Madrid, Spain

SUPPLEMENTARY INFORMATION

S1. STARTING MATERIALS AND SYNTHESIS

S1.1. Materials and reagents

All reagents and solvents employed were commercially available and used as received without further purification: $Zn(NO_3)_2 \cdot 6H_2O$ (98,5% Scharlau); $MnCl_2 \cdot 4H_2O$ (>98% Probus); $Co(NO_3)_2 \cdot 6H_2O$ (>97,7% Alfa Aesar) $Ca(NO_3)_2 \cdot 4H_2O$ (≥99% Sigma Aldrich); 4,4'-(hexafluoroisopropylidene)bis(benzoic acid), $H_2hfipbb$ (>98% TCI); HNO_3 (65%, Labkem) and absolute ethanol (Scharlau).

S1.2. Synthesis of MM-MTV-MOFs.

Multimetal multivariate metal-organic frameworks (MM-MTV-MOFs) synthesis was based on the original previously reported procedure[1]. For the preparation of all MM-MTV-MOFs, a general synthetic procedure was followed, in which the organic linker and the metal salts were dissolved in a water:ethanol:HNO_3 mixture, followed by heating at 170 ºC overnight. The synthesis procedure is illustrated here for the $Zn_{0.16}Mn_{0.47}Co_{0.33}Ca_{0.03}(hfipbb)$ compound:

A mixture of $Zn(NO_3)_2 \cdot 6H_2O$ (10.0 mg, 0.033 mmoles), $MnCl_2 \cdot 4H_2O$ (26.0 mg, 0.132 mmol), $Co(NO_3)_2 \cdot 6H_2O$ (38.0 mg, 0.132 mmol), $Ca(NO_3)_2 \cdot 4H_2O$ (8.0 mg, 0.033 mmol) and $H_2hfipbb$ (78.0 mg, 0.200 mmol) were dissolved in a solvent mixture of 5 mL of distilled water, 5 mL of absolute ethanol and 300 μL of a 1M HNO_3 solution. In order to facilitate the dissolution of the reagents and achieve homogeneity of the mixture, the solution was stirred at room temperature for 5 minutes. Subsequently, the mixture was placed in a Teflon-lined steel autoclave and heated at 170 °C overnight.

Once the reaction had cooled to room temperature, the blue needle-shaped crystals were separated by filtration and washed with water and acetone before being dried under vacuum. The rest of the materials were similarly prepared, using the amounts of metal salts specified in Table S1, while maintaining the same proportions of linker and solvents.

Table S1. Chemical formulas, corresponding starting molar codes and amount of metal salts used for MM-MTV-MOFs preparation.

Entry	Compound	Molar code				$Zn(NO_3)_2 \cdot 6H_2O$	$MnCl_2 \cdot 4H_2O$	$Co(NO_3)_2 \cdot 6H_2O$	$Ca(NO_3)_2 \cdot 4H_2O$
		Zn	Mn	Co	Ca	mg (mmol)	mg (mmol)	mg (mmol)	mg (mmol)
1	$Zn_{0.16}Mn_{0.47}Co_{0.33}Ca_{0.03}$(hfipbb)	1	4	4	1	10 (0.033)	26 (0.132)	38 (0.132)	8 (0.033)
2	$Zn_{0.37}Mn_{0.28}Co_{0.13}Ca_{0.22}$(hfipbb)	1	1	1	7	10 (0.033)	7 (0.033)	10 (0.033)	55 (0.231)
3	$Zn_{0.46}Mn_{0.21}Co_{0.17}Ca_{0.15}$(hfipbb)	2	1	2	2	28 (0.094)	9 (0.047)	27 (0.094)	22 (0.094)

S2. CHARACTERIZATION

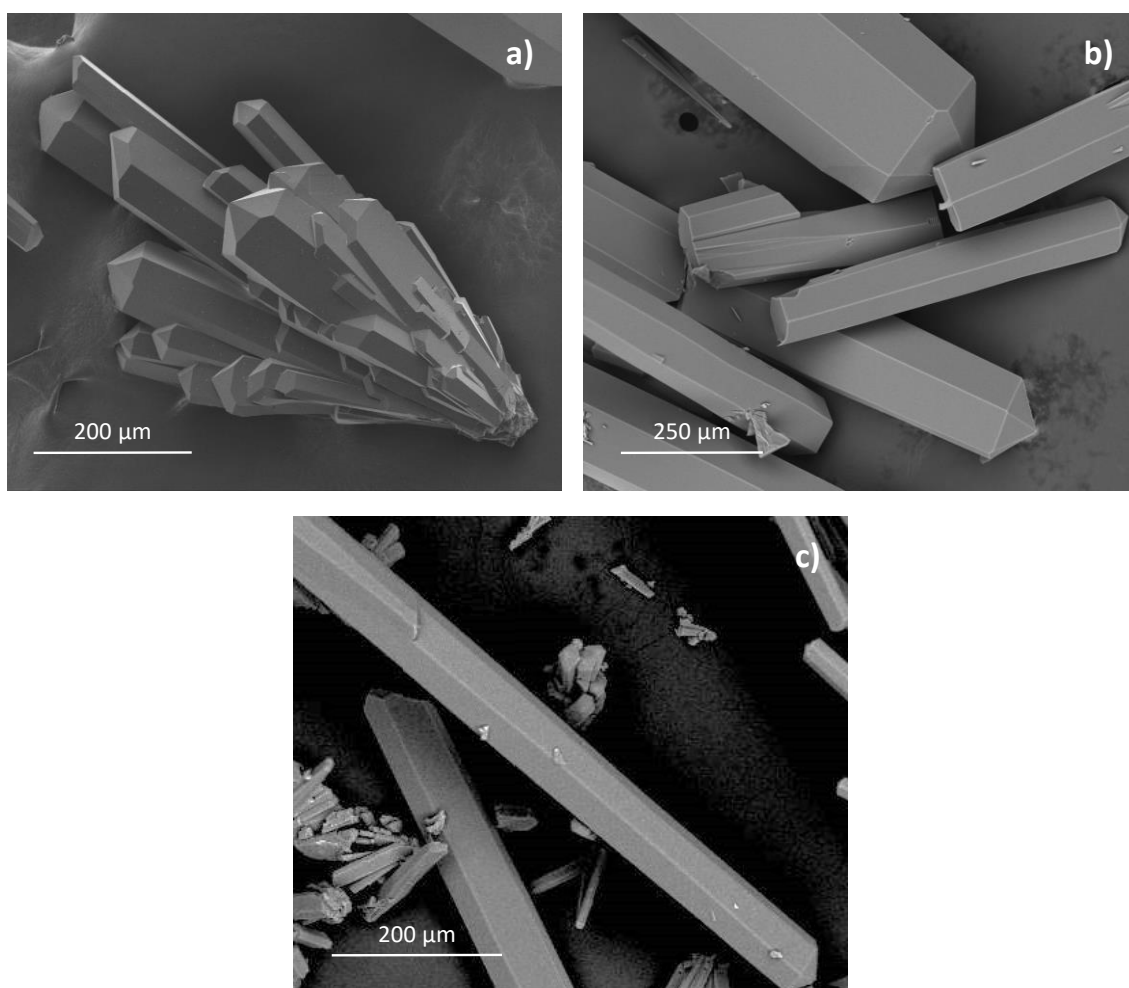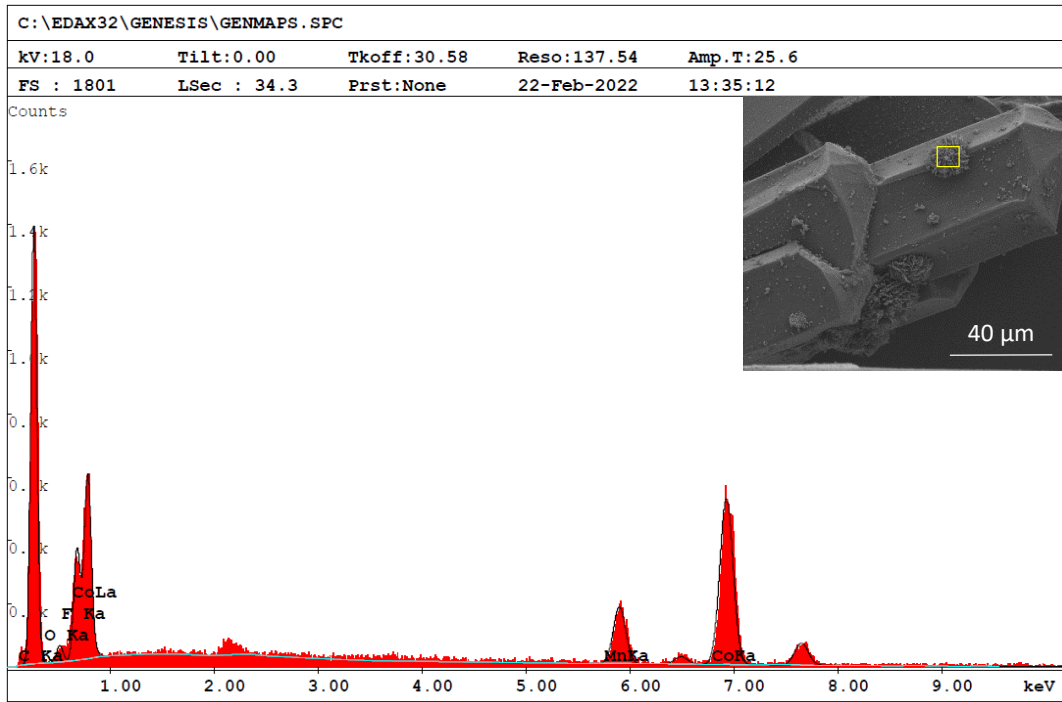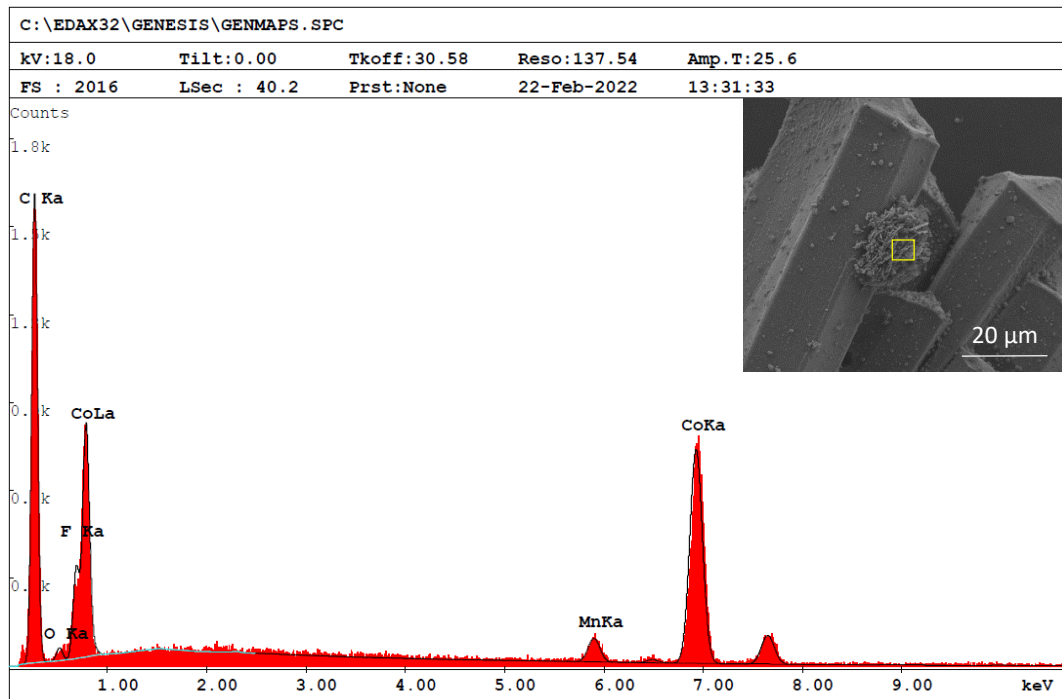### S2.1.   Scanning Electron Microscopy (SEM-EDX)

Figure S1. SEM images of the precursor MM-MTV-MOFs for MODEs (a) 1441, (b) 1117 and (c) 2122.

a)

C:\EDAX32\GENESIS\GENMAPS.SPC

kV:18.0	Tilt:0.00	Tkoff:30.58	Reso:137.54	Amp.T:25.6
FS : 1801	LSec : 34.3	Prst:None	22-Feb-2022	13:35:12

Counts

1.6k

1.4k

1.2k

1.0k

0. k

0. k

0. k

CoLa
F Ka
O Ka
C Ka

MnKa   CoKa

40 μm

1.00   2.00   3.00   4.00   5.00   6.00   7.00   8.00   9.00   keV

b)

C:\EDAX32\GENESIS\GENMAPS.SPC

kV:18.0	Tilt:0.00	Tkoff:30.58	Reso:137.54	Amp.T:25.6
FS : 2016	LSec : 40.2	Prst:None	22-Feb-2022	13:31:33

Counts

1.8k

C Ka

1. k

1. k

0. k   CoLa

F Ka

0. k

0. k   O Ka

CoKa

MnKa

20 μm

1.00   2.00   3.00   4.00   5.00   6.00   7.00   8.00   9.00   keV

c)


```
C:\EDAX32\GENESIS\GENMAPS.SPC
kV:18.0        Tilt:0.00        Tkoff:30.58    Reso:137.54    Amp.T:25.6
FS : 1382      LSec : 30.1      Prst:None      22-Feb-2022    13:32:48
```

Counts

1.2k

C Ka

1.0k

0. k

0. k

0. k

F Ka

MnKa

0. k

CoLa

CoKa

O Ka

20 μm

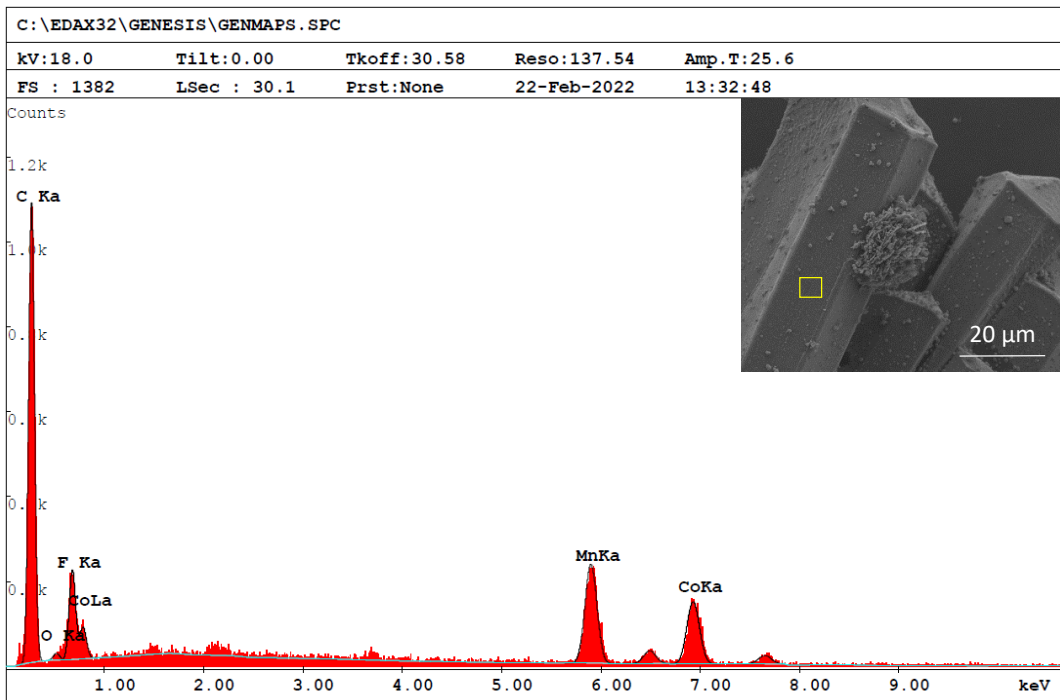1.00   2.00   3.00   4.00   5.00   6.00   7.00   8.00   9.00   keV

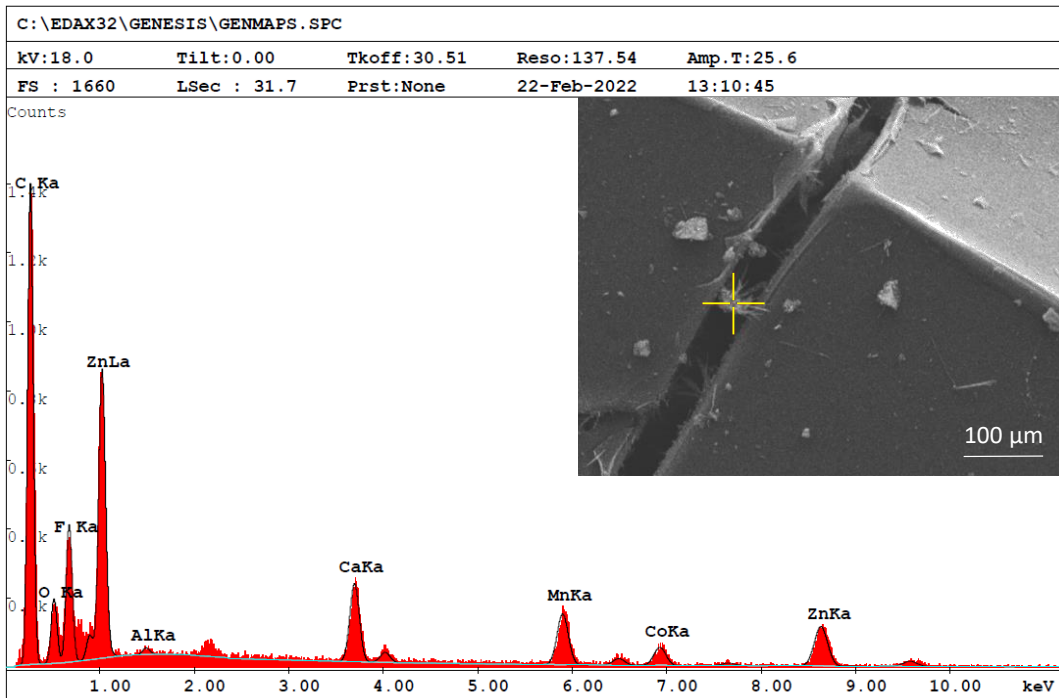*Figure S2. a-c) EDX analysis and SEM images for different MODE-1441 samples.*

S4
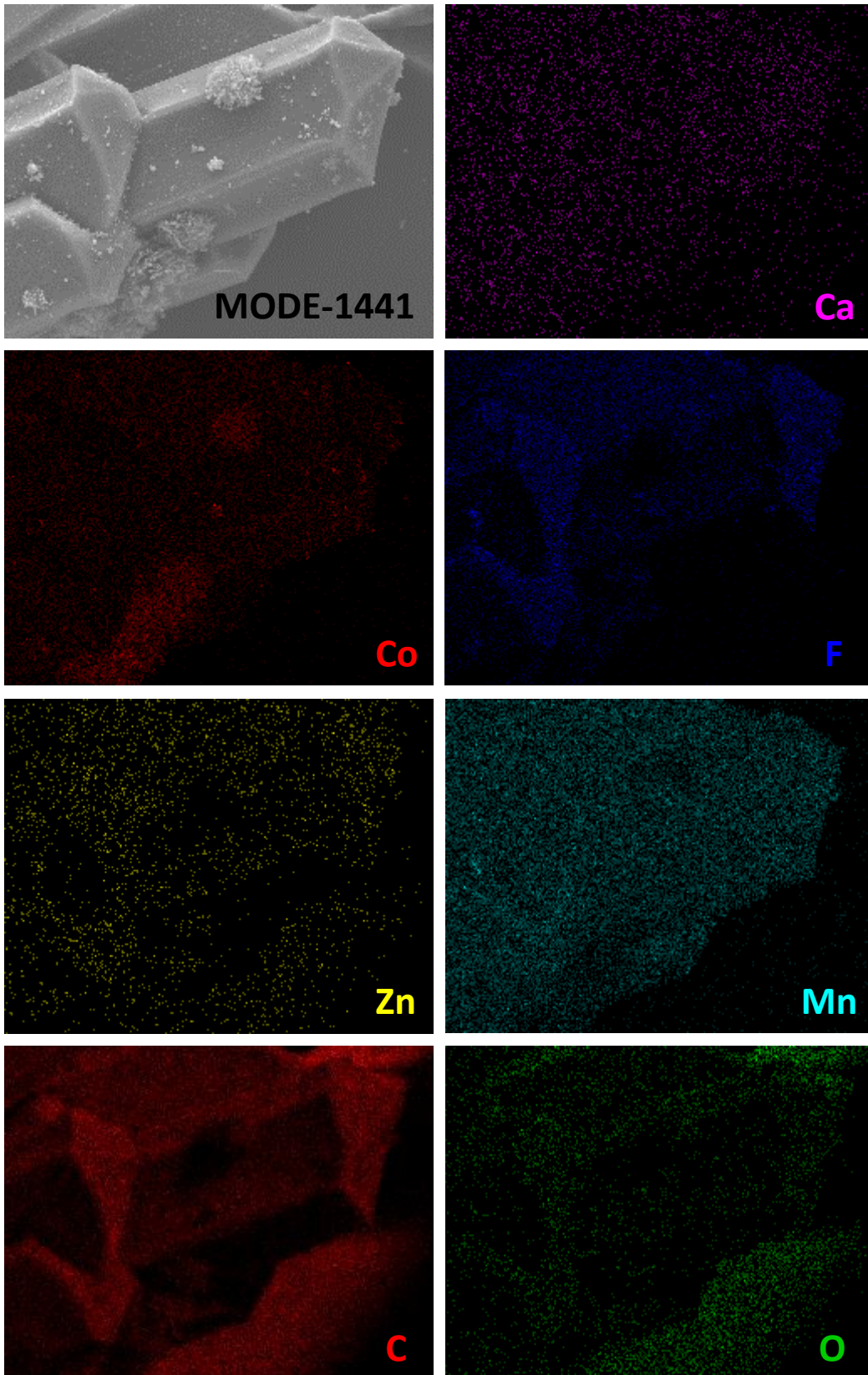
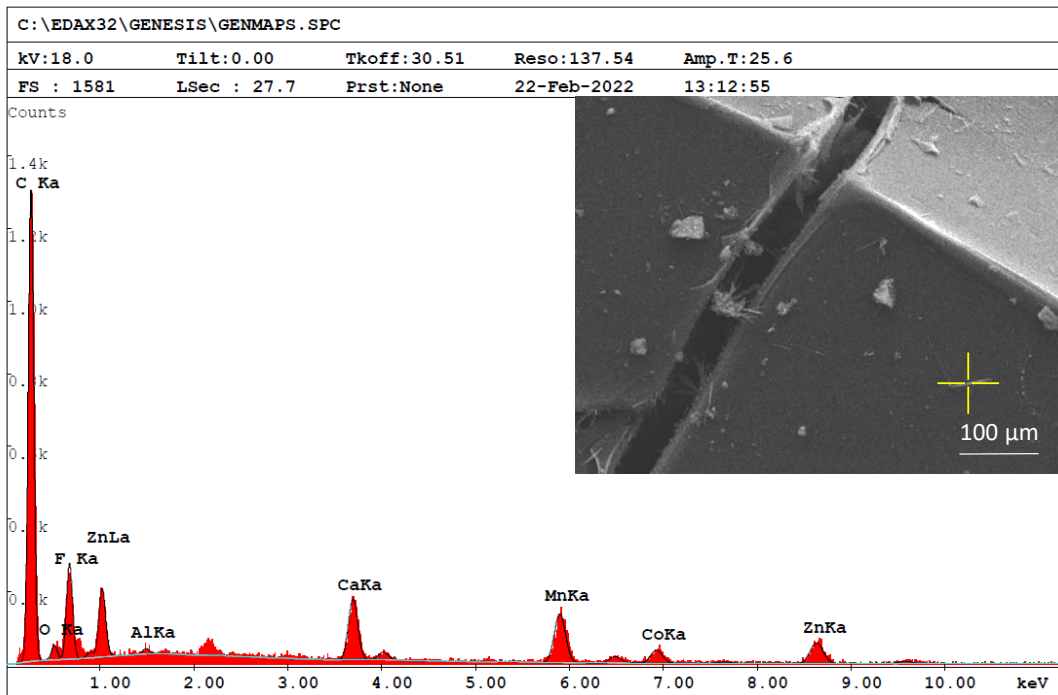*Figure S3. EDX mapping for MODE-1441 sample.*

a)
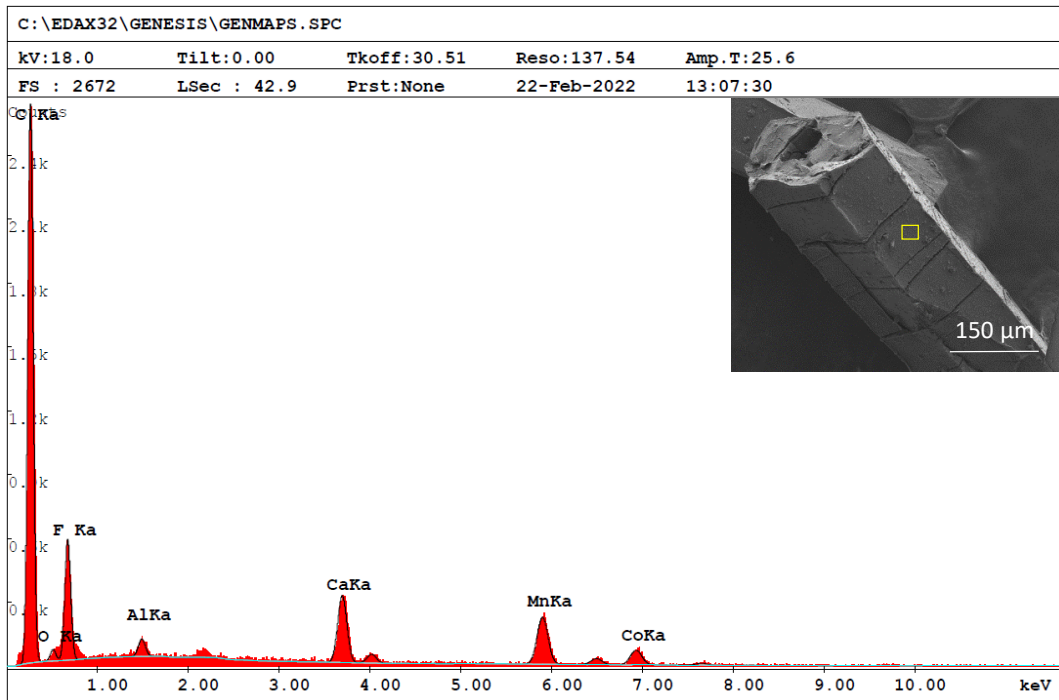
b)

c)

Figure S4. a-c) EDX analysis and SEM images for different MODE-1117 samples.
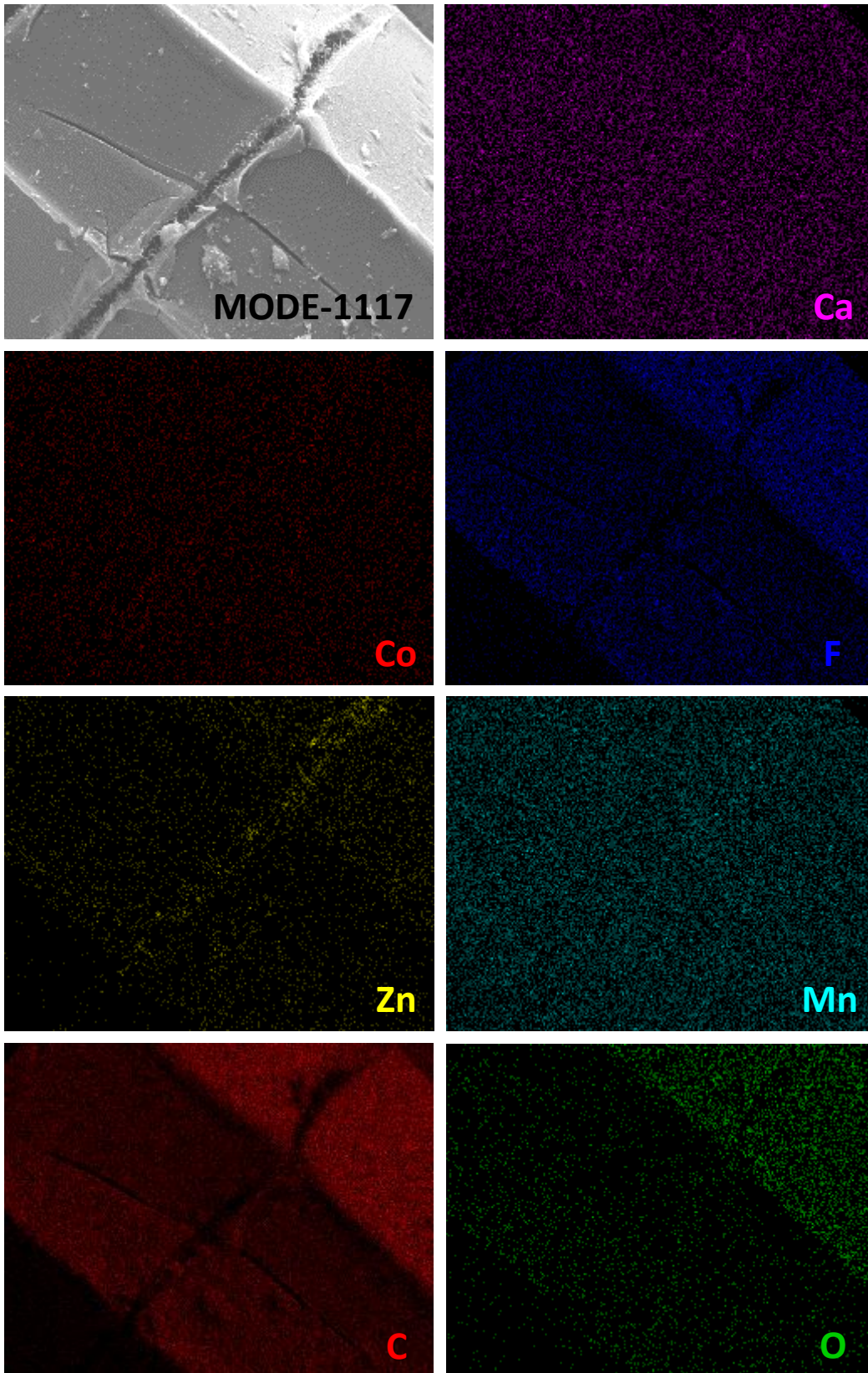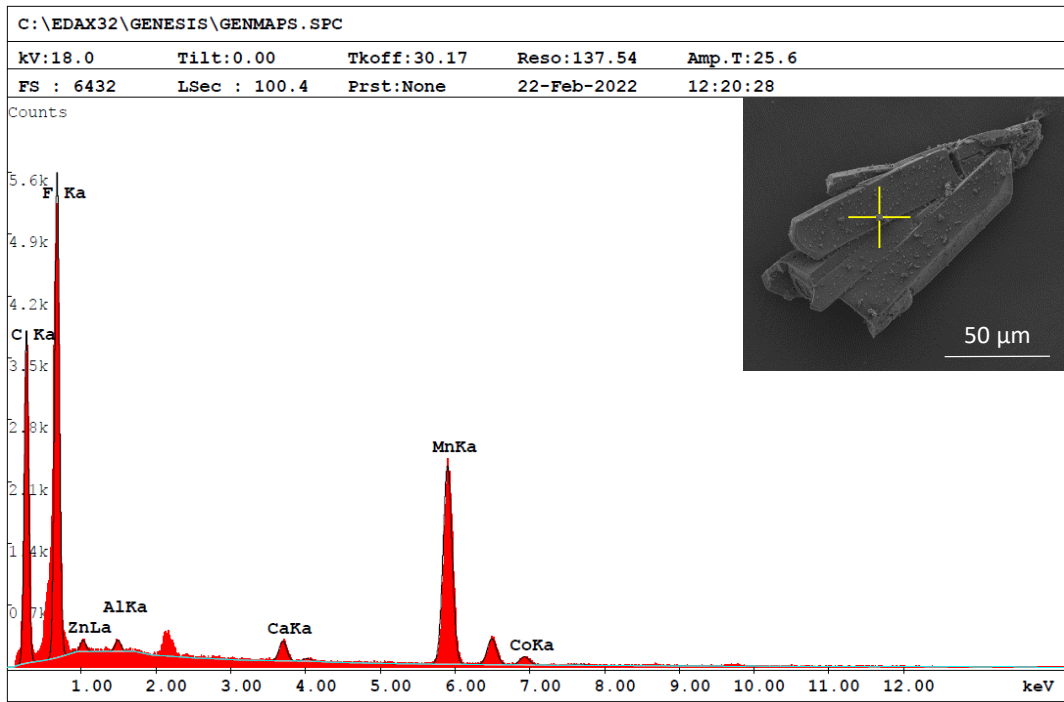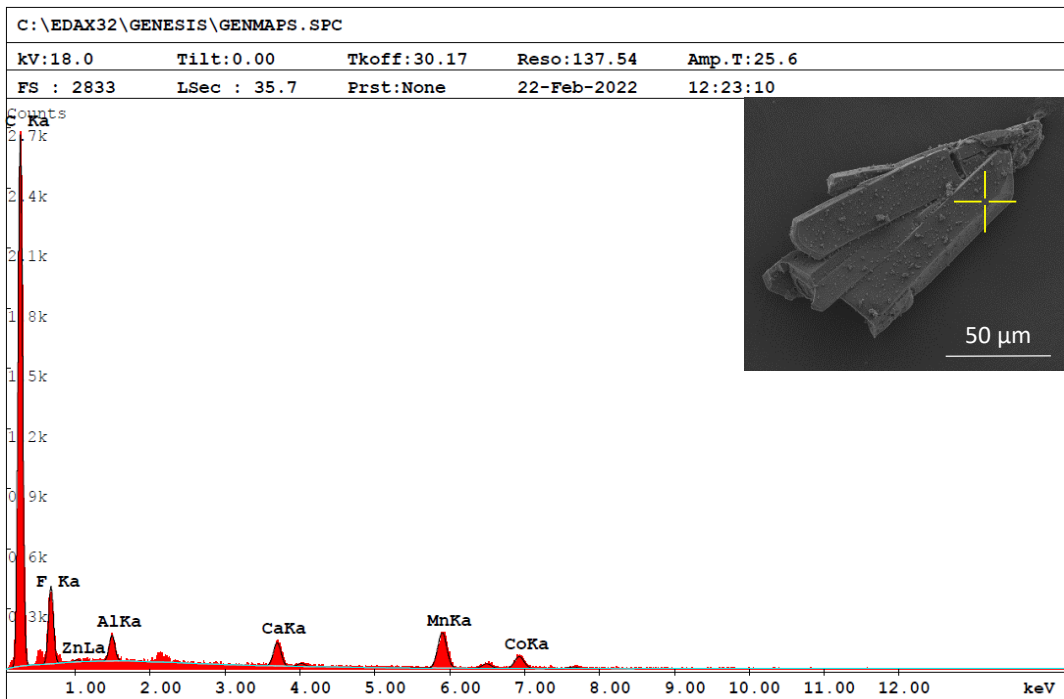
Figure S5. EDX mapping for MODE-1117 sample.
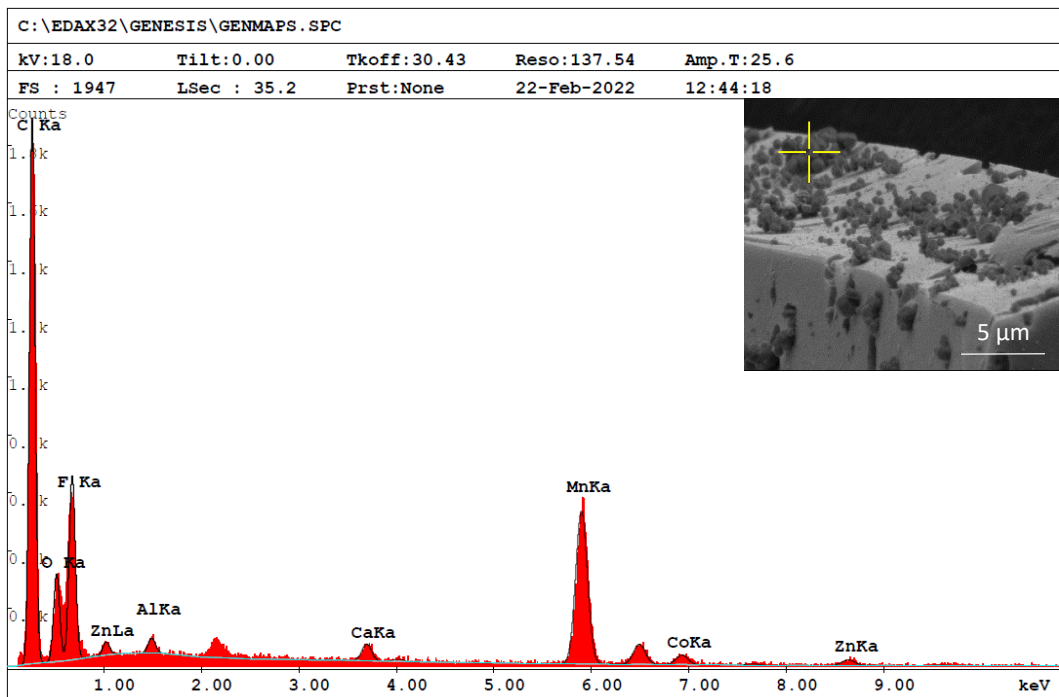
a)

b)

c)

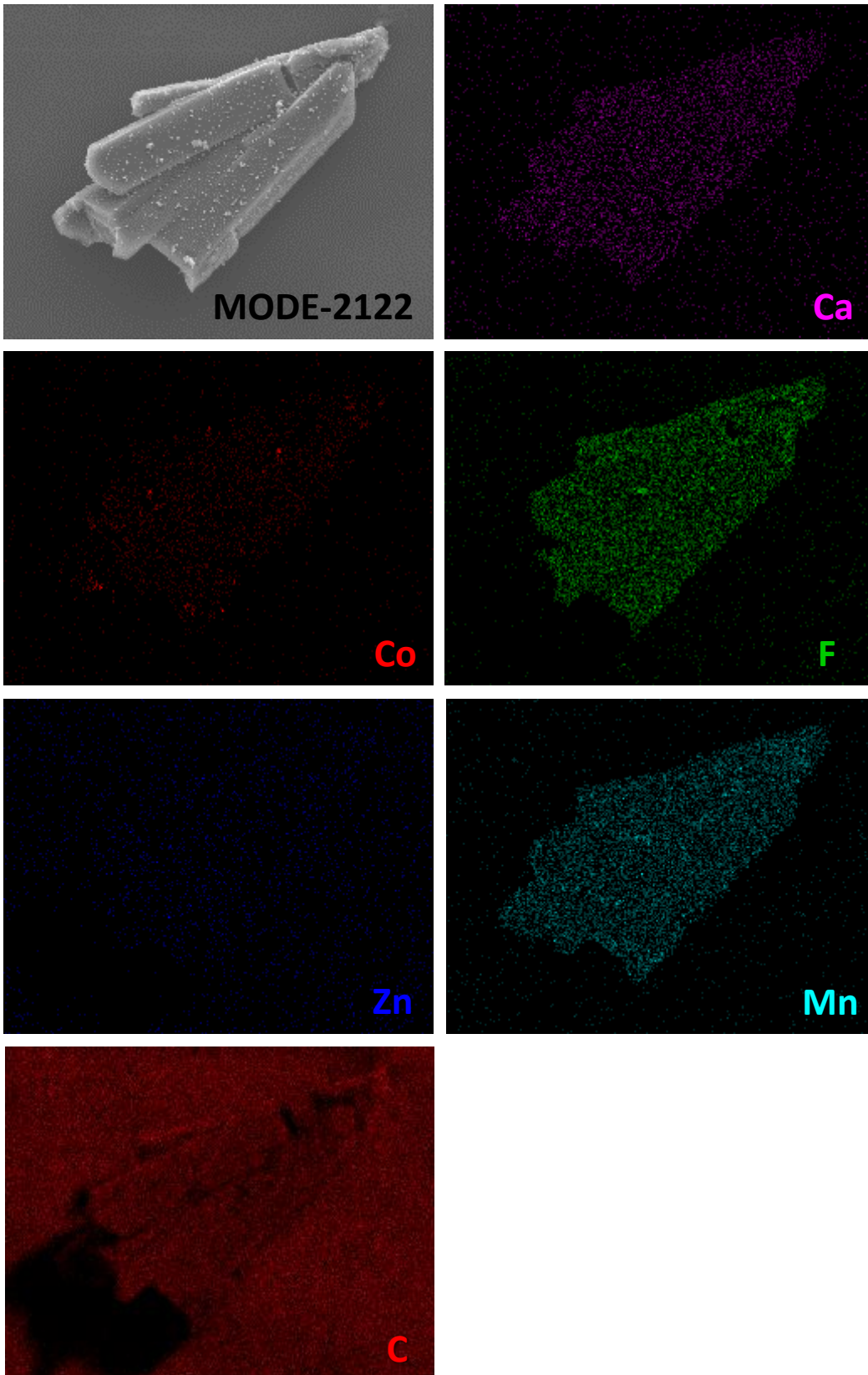*Figure S6. a-c) EDX analysis and SEM images for different MODE-2122 samples.*

Figure S7. EDX mapping for MODE-2122 sample.

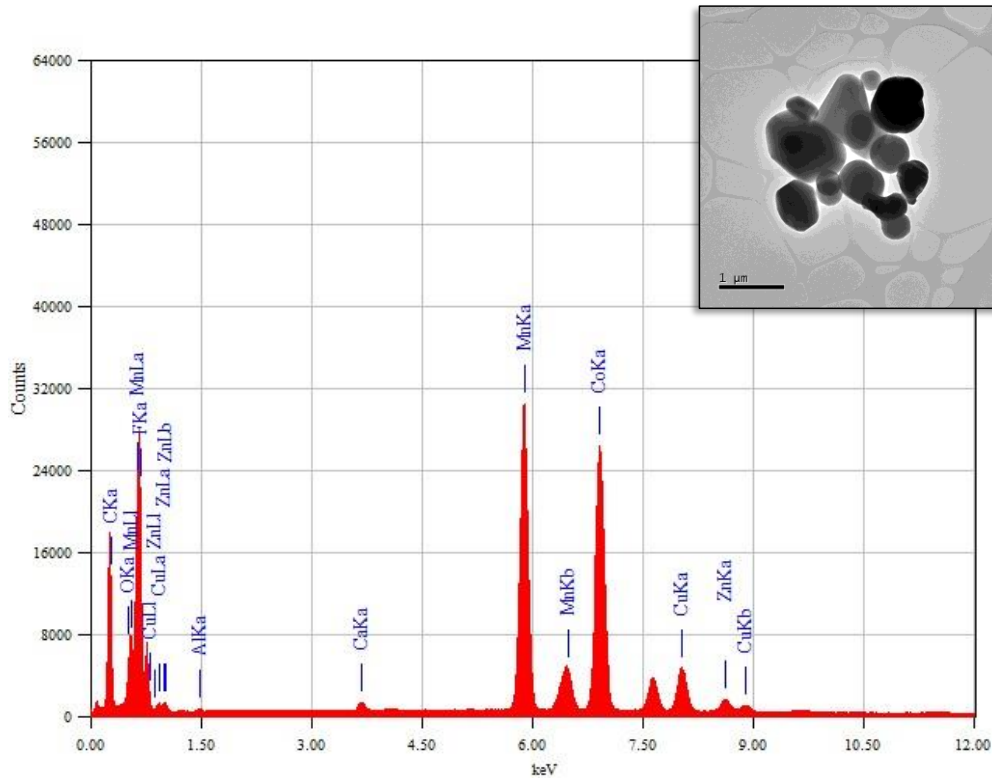## S2.2.   Transmission Electron Microscopy (TEM-EDX)

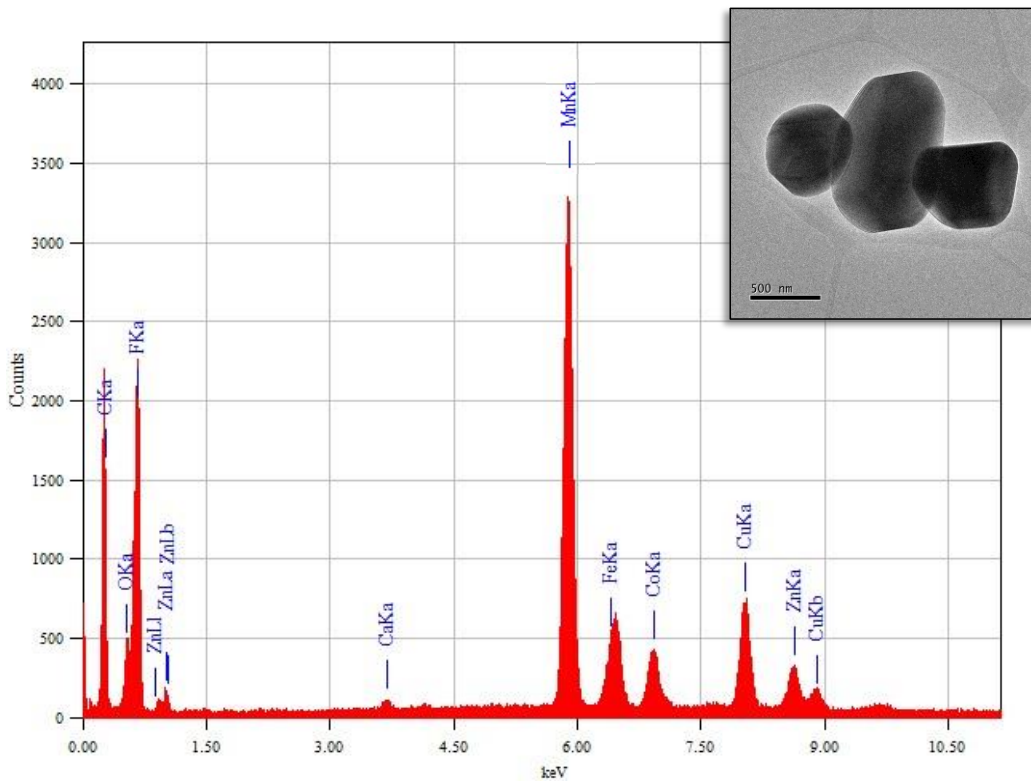*Figure S8. EDX analysis and TEM image for MODE-1441.*

Figure S9. EDX analysis and TEM image for MODE-1441.
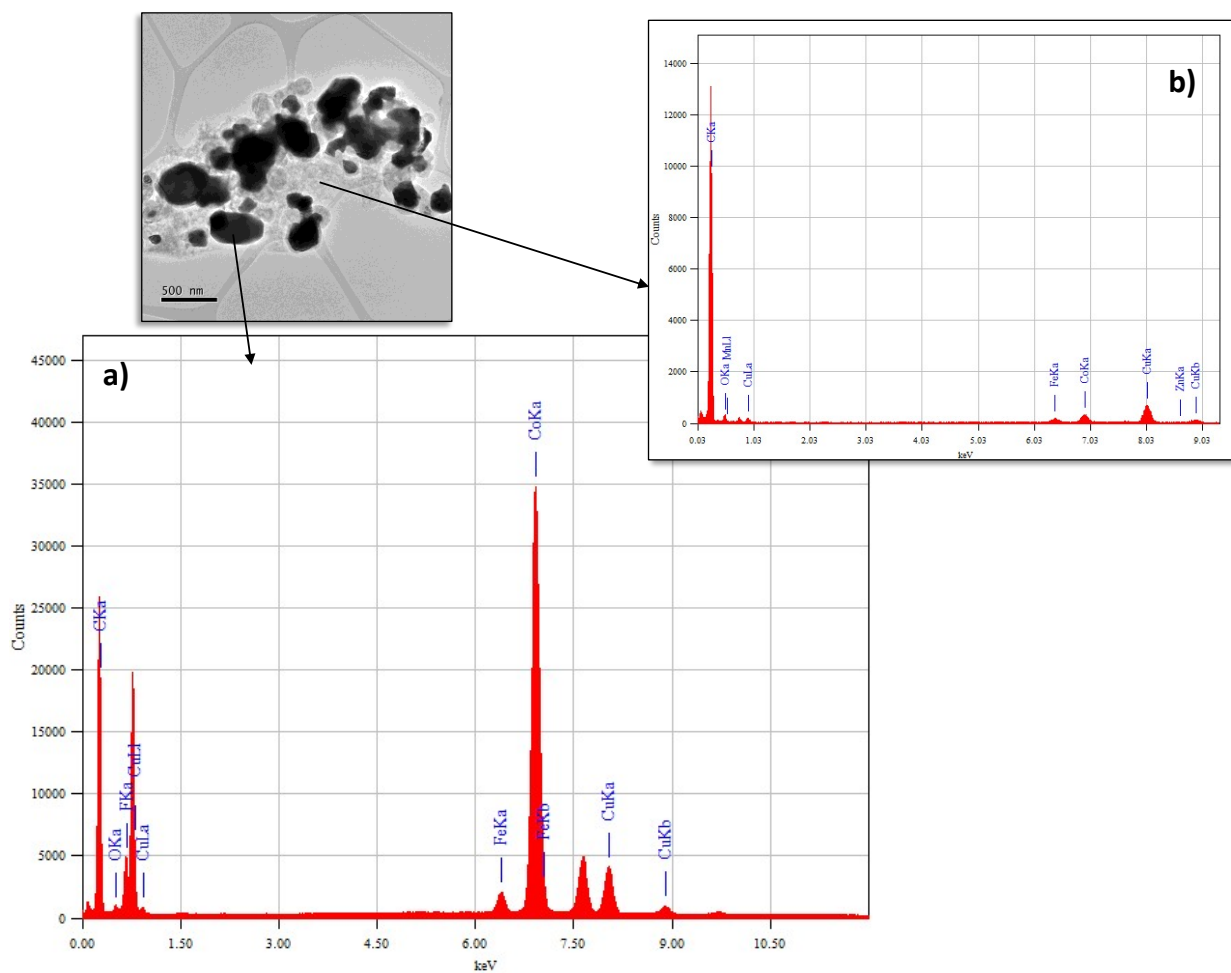
Figure S10. a,b)EDX analysis and TEM image for MODE-1441.
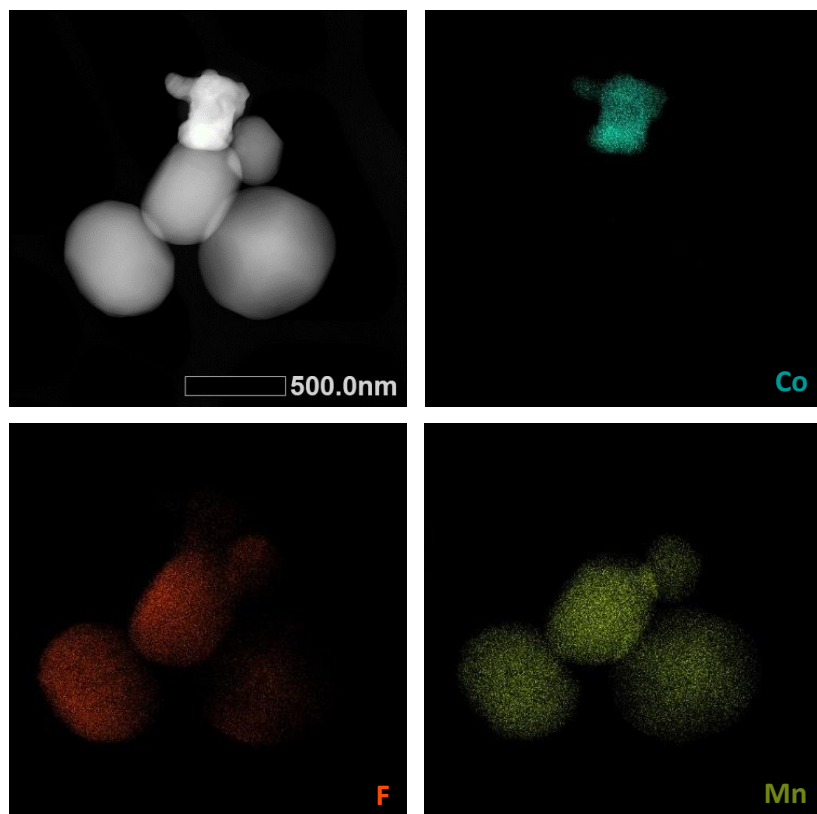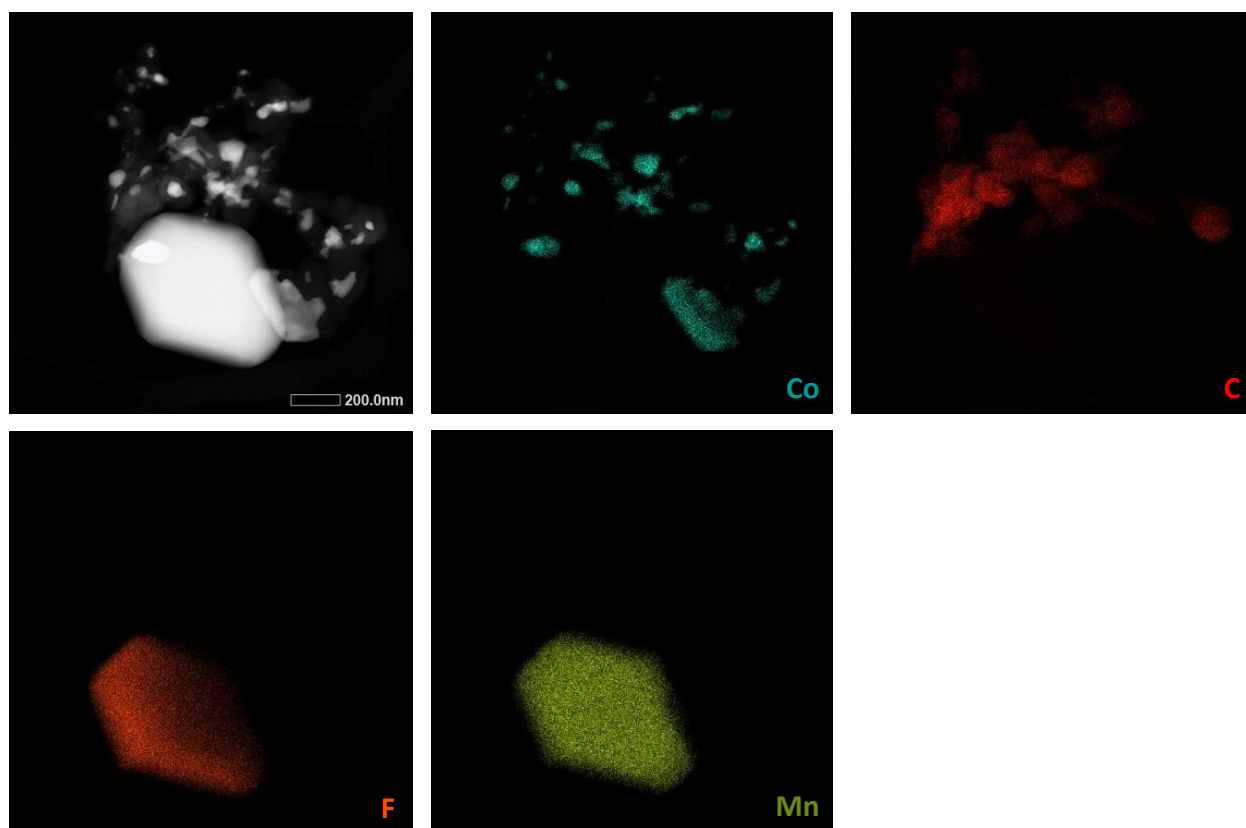
Figure S11. EDX mapping for MODE-1441 sample.

Figure S12. EDX mapping for MODE-1441 sample.

S3. PHOTOCATALYTIC ACTIVITY STUDIES

S3.1.   Photoreactor details

The photoreactor employed in all the tests conducted for the purpose of studying MODEs activity for dye photodegradation comprises a circular metal container with a lid, into which the light source and the adapter holder are placed, as seen in Figure S13. The light source is a LED light ring emitting blue light at a wavelength of 440 nm, which is concentric to the holder for vials. This configuration ensures that a source-sample distance of 3 cm is maintained for all experiments. Furthermore, the photoreactor is situated on a magnetic stirring plate, which ensures continuous agitation.
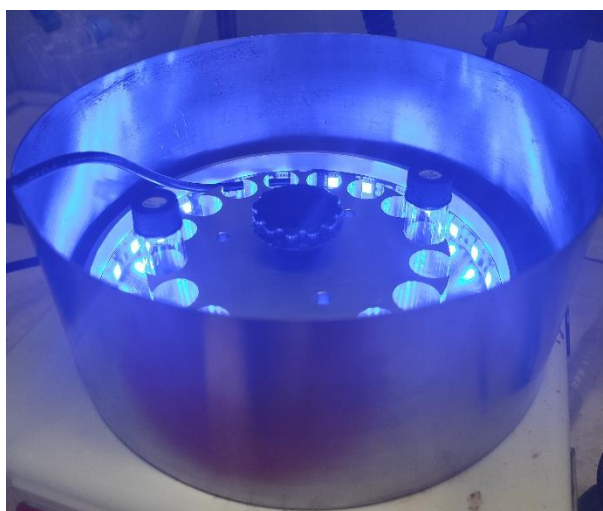
Figure S13. Photoreactor detailed setup for MODEs dye photodegradation studies.

S3.2.   Dyes photodegradation

The pH of the organic solution of the selected pollutant has a noticeable impact on the degradation rate. With regard to methyl orange, previous studies have determined the influence of this factor in photocatalytic reactions similar to those proposed in this work, using different metal oxides. These studies have demonstrated that the optimal pH for the photodegradation of methyl orange is near pH 7.[2–5] In our case, the studies were conducted at pH 6 which is no far from the optimal value.

Reproducibility tests were conducted for the best performing material (MODE-1441), confirming the same degradation values (98% and 99% for MO, and 99% and 99% for MR).

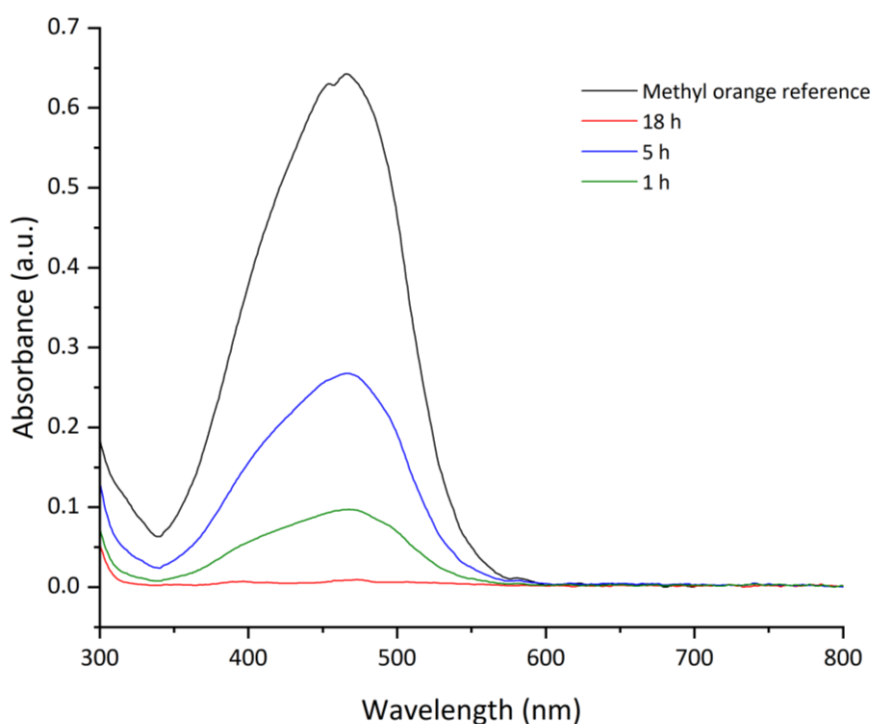### S3.2.1. MODEs photocatalytic activity

Figure S14. Comparative graph for original signal of methyl orange (black), and its signal after photocatalysis reaction under oxygen, blue light and MODE-2122 for 18 h (red), 5 h (blue) and 1 h (green).

Figure S15. Comparative graph for original signal of methyl orange (black), and its signal after photocatalysis reaction under oxygen, 18 h and blue light using MODE-1441 (blue) and its MM-MTV-MOF precursor, $Zn_{0.16}Mn_{0.47}Co_{0.33}Ca_{0.03}$(hfipbb) (red).
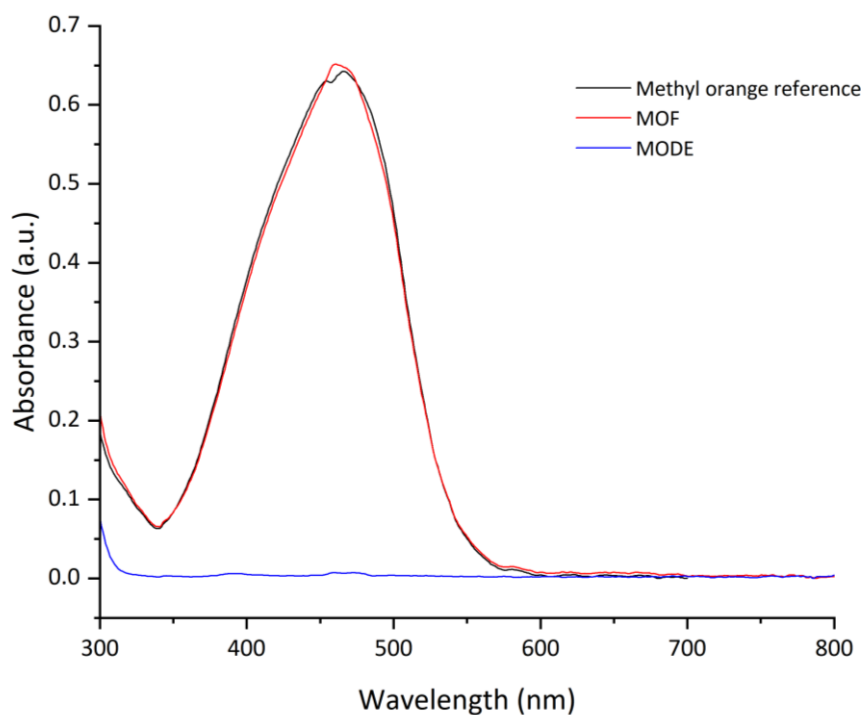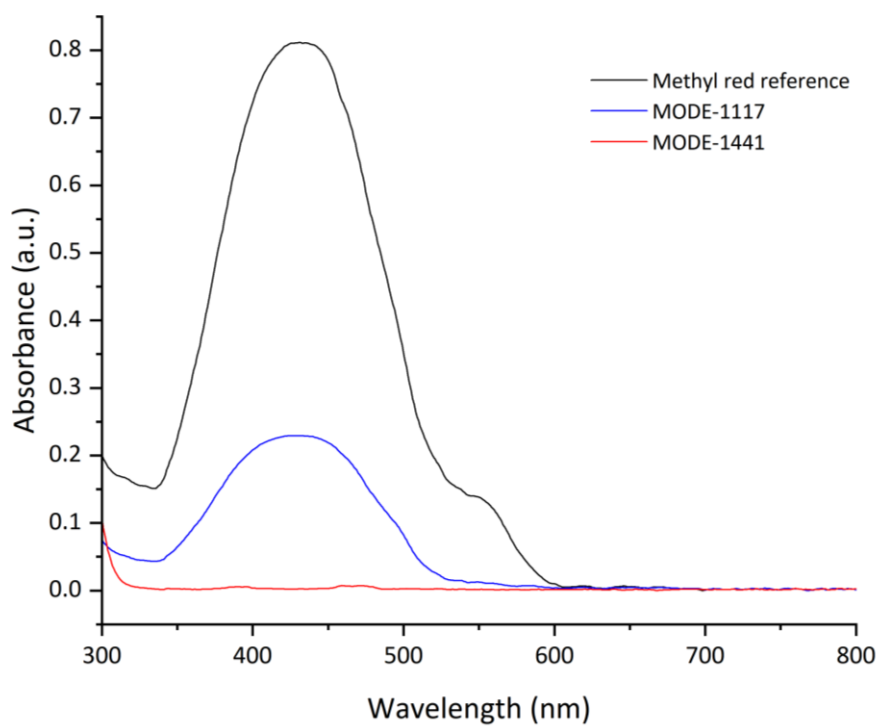

Figure S16. Comparative graph for original signal of methyl red (black), and its signal after photocatalysis reaction under oxygen, 18 h and blue light using MODE-1441 (red) and MODE-1117 (blue).

S3.2.2. MODOs photocatalytic activity

The procedure for the obtention of MOF-derived oxides (MODOs) was based on the original previously reported method.[1] All studies conducted for MODOs dye photodegradation activity were performed in accordance with the same methodology and under identical conditions as those employed for the MODEs. All the materials tested are detailed in Table S2.

The resulting UV-Vis spectra obtained for all the photocatalytic activity studies of the different MODOs are presented in Figure S17. The corresponding formulas and color code for the MODOs are listed in the guide inserted on the figure. The MODOs tested for this study were found to be ineffective under the conditions previously described for the photodegradation of methyl orange.

Table S2. Starting molar codes, corresponding MOFs and MODOs formula studied for dye photodegradation

| Entry	Molar code				MOF formula	MODO formula
	Zn	Mn	Co	Ca		
1	1	1	1	1	$Zn_{0.42}Mn_{0.42}Co_{0.11}Ca_{0.06}(hfipbb)$	$Zn_{1.26}Mn_{1.26}Co_{0.33}Ca_{0.18}O_4$
2	1	1	4	4	$Zn_{0.18}Mn_{0.24}Co_{0.41}Ca_{0.16}(hfipbb)$	$Zn_{0.54}Mn_{0.72}Co_{1.23}Ca_{0.48}O_4$
3	1	4	4	4	$Zn_{0.24}Mn_{0.37}Co_{0.31}Ca_{0.08}(hfipbb)$	$Zn_{0.72}Mn_{1.11}Co_{0.93}Ca_{0.24}O_4$
4	1	4	1	4	$Zn_{0.32}Mn_{0.40}Co_{0.15}Ca_{0.12}(hfipbb)$	$Zn_{0.96}Mn_{1.20}Co_{0.45}Ca_{0.36}O_4$
5	1	1	7	1	$Zn_{0.13}Mn_{0.27}Co_{0.52}Ca_{0.03}(hfipbb)$	$Zn_{0.39}Mn_{0.81}Co_{1.56}Ca_{0.09}O_4$
6	1	3	9	0	$Zn_{0.12}Mn_{0.42}Co_{0.46}(hfipbb)$	$Zn_{0.36}Mn_{1.26}Co_{1.38}O_4$
7	1	12	6	0	$Zn_{0.17}Mn_{0.45}Co_{0.38}(hfipbb)$	$Zn_{0.51}Mn_{1.35}Co_{1.14}O_4$
8	1	10	20	0	$Zn_{0.10}Mn_{0.40}Co_{0.50}(hfipbb)$	$Zn_{0.30}Mn_{1.20}Co_{1.50}O_4$
9	0	1	2	2	$Mn_{0.23}Co_{0.50}Ca_{0.27}(hfipbb)$	$Mn_{0.69}Co_{1.50}Ca_{0.81}O_4$
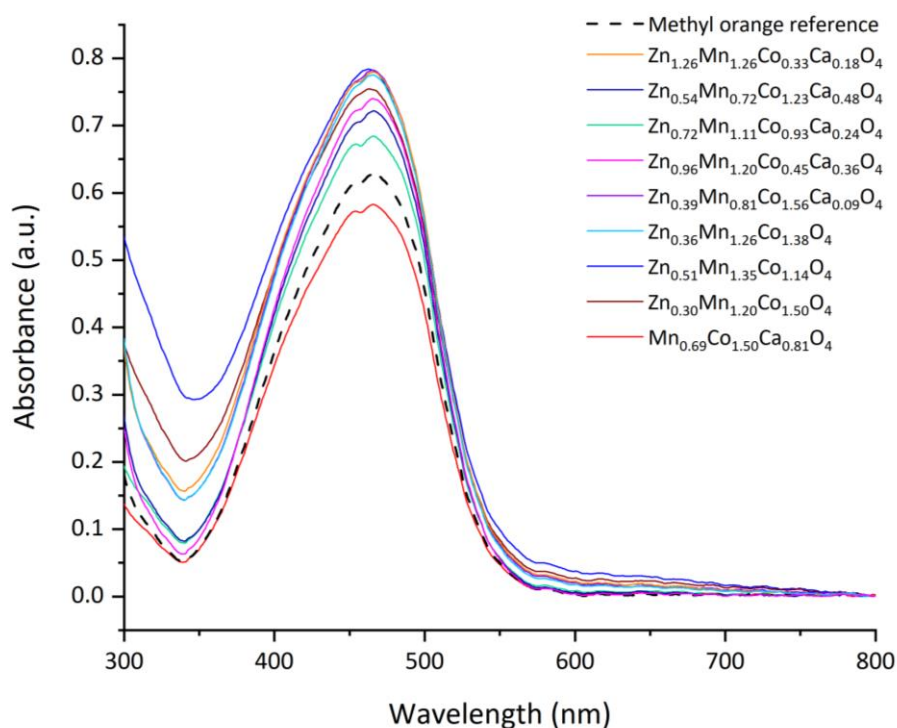
Figure S17. UV-Vis spectra obtained for MODOs photocatalytic activity studies. The corresponding MODOs formulas and color codes are listed in the guide inserted on the graph.

S3.3.   Paracetamol photodegradation

The initial studies of paracetamol (PMA) photodegradation in water using MODE-1441 as a catalyst, a consistent procedure was employed in all cases, with the exception of experiments that did not require the addition of H_2SO_4. In a clear vial, 8 mg of the catalyst (MODE-1441), 4 mL of an aqueous solution of PMA 1000 ppm and 100 μL of H_2SO_4 1M were added. The mixture was stirred at room temperature, under purple light (405 nm) and air atmosphere for 18 hours. A pH value of 3.0 was selected as the optimal parameter based on the findings of prior studies on photocatalytic procedures.[6,7]

To analyse the results, a 10000 ppm naphthol (NPh) solution was employed as an external standard.
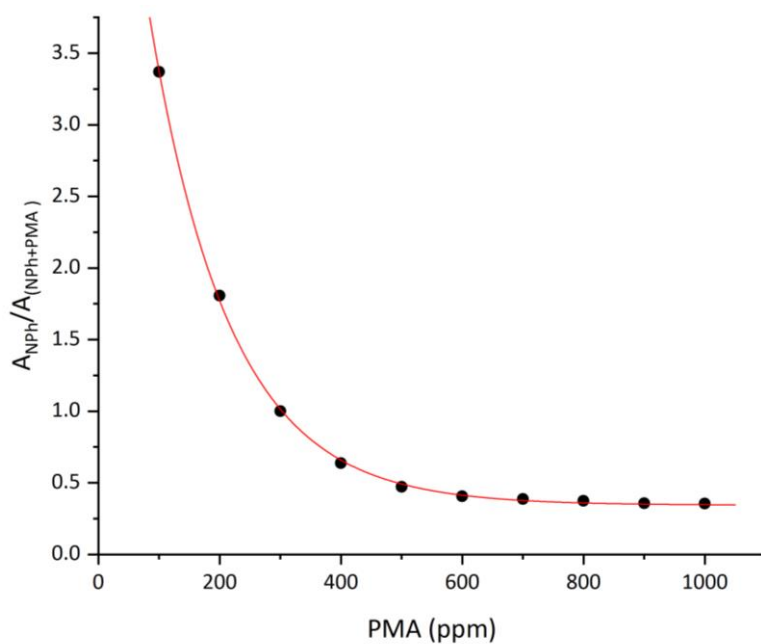
Figure S18. Graphical representation of the data fitting equation for paracetamol photodegradation studies by HPLC.

Table S3. HPLC data results for photodegradation of PMA under air, 18 h and purple light using MODE-1441 as catalyst.

Entry	H_2SO_4 1M (µL)	Catalyst (mg)	A_{NPh}	$A_{(NPh+PMA)}$	$A_{NPh}/A_{(NPh+PMA)}$	C_{final} PMA (ppm)	Degradation PMA (%)
1	100	-	121.6	318.8	0.38	669.3	16.3
2	-	-	124.1	340.4	0.36	738.3	7.7
3	100	8	124.2	276.8	0.45	541.2	45.9
4	-	8	130.2	355.7	0.37	730.6	26.9

S4. REFERENCES

1   C. Castillo-Blas, N. López-Salas, M. C. Gutiérrez, I. Puente-Orench, E. Gutiérrez-Puebla, M. L. Ferrer, M. Á. Monge and F. Gándara, *J. Am. Chem. Soc.*, 2019, **141**, 1766–1774.

2   C. Chen, J. Liu, P. Liu and B. Yu, *Adv. Chem. Eng. Sci.*, 2011, **01**, 9–14.

3   A. Zyoud, A. Zu'bi, M. H. S. Helal, D. Park, G. Campet and H. S. Hilal, *J. Environ. Heal. Sci. Eng.*, 2015, **13**, 46.

4   S. F. Bdewi, A. M. Abdulrazaka and B. K. Aziz, *Asian Trans. Eng.*, 2015, **5**, 1–5.

5   M. Sadia, A. Saqib, J. Khan, M. Zahoor and I. Zekker, *Desalin. WATER Treat.*, 2022, **262**, 256–265.

6   J. Medina-Valtierra, E. Moctezuma, M. Sánchez-Cárdenas and C. Frausto-Reyes, *J. Photochem. Photobiol. A Chem.*, 2005, **174**, 246–252.

7   G. E. do Nascimento, M. A. Soares Oliveira, R. M. da Rocha Santana, B. G. Ribeiro, D. C. Silva Sales, J. M. Rodríguez-Díaz, D. C. Napoleão, M. A. da Motta Sobrinho and M. M. M. B. Duarte, *Water Sci. Technol.*, 2020, **81**, 2545–2558.